

## Scattering on the lateral one-dimensional superlattice with spin-orbit coupling

D. V. Khomitsky

Department of Physics, University of Nizhny Novgorod,  
23 Gagarin Avenue, 603950 Nizhny Novgorod, Russian Federation

(Dated: December 18, 2019)

The problem of scattering of the two-dimensional electron gas on the lateral one-dimensional superlattice both having different strengths of Rashba spin-orbit coupling is investigated. The scattering is considered for all the electron states on a given Fermi level. The distribution of spin density components along the superlattice is studied for the transmitted states where the formation of standing waves is observed. It is found that the shape of spin density distribution is robust against the variations of the Rashba coupling constants, the superlattice potential strength, and the Fermi level in the electron gas.

PACS numbers: 72.25.Dc, 72.25.Mk, 73.21.Cd

## I. INTRODUCTION

In two-dimensional semiconductor heterostructures the spin-orbit (SO) interaction is usually dominated by the Rashba coupling<sup>1</sup> coming from the structure inversion asymmetry of conning potential and effective mass difference. The interest to these structures is usually related to the possible effects in charge and spin transport which produce novel ideas on the spin control in semiconductor structures and give rise to the applications of spintronics.<sup>2</sup> One of the first possible applications was the principle of the spin field-effect transistor proposed by Datta and Das<sup>3</sup> who investigated the ballistic transport of spin-polarized electrons through quasione-dimensional (1D) channel composed of a series of segments with and without SO interaction. They considered the lateral interface between two regions with different strengths of the spin-orbit interaction which can be used to control the electron spin in gated two-dimensional semiconductor heterostructures. For a beam with a nonzero angle of incidence, the transmitted electrons will split into two spin polarization components propagating at different angles. Later, the low-dimensional semiconductor structures with SO interaction were studied theoretically in numerous papers<sup>4,5,6,7,8,9,10,11,12,13</sup> including the 1D periodic systems with SO coupling.<sup>8,9,11,12</sup> In particular, the ballistic spin transport through the electron waveguides with periodically modulated geometrical parameters<sup>8</sup> and spin-orbit coupling strength<sup>9,12</sup> has been studied, and for the latter case the transmission coefficient has been calculated.<sup>9,12</sup> One of the most interesting parameters of two-dimensional electron gas (2DEG) with SO interaction is the space distribution of the spin density components which was studied, for example, in a problem of 2DEG scattering at the edges of the sample, where it demonstrates an oscillating shape.<sup>13</sup> It should be mentioned that the strength of Rashba SO coupling in a gated structure can be modulated by the external gate potential for up to 50%<sup>14</sup> which makes reasonable the investigation of gated structures with varying SO strength.

The (2DEG) with SO interaction was also studied in the presence of the magnetic field. In particular, the band

structure and magnetotransport of the electron gas were studied for both Rashba and Dresselhaus SO interaction terms<sup>7</sup>. The quantum states of the electron gas with the SO interaction were also investigated in the presence of 2D superlattice potential<sup>15</sup> and the magnetocconductivity oscillations in the SO electron system were calculated for the 2DEG subject to the 1D superlattice potential.<sup>16</sup>

The idea to control the spin orientation in the beam of particles by means of SO coupling has been proposed also in terms of spin optics.<sup>17,18</sup> In particular, the scattering on the border of two half-spaces each having a different value of SO coupling constants was studied.<sup>17</sup> It was shown that the spin orientation in transmitted wave strongly depends on the chirality of the incident one as well as on the angle of incidence and the angles of total reflection exist. Later the same authors applied their results for the case of spin polarizing in a system consisted of ballistic and diffusive regions.<sup>18</sup> Nowadays the problem of new structures and schemes to be proposed for the application of SO interaction for control of the spin degrees of freedom without applying the external magnetic field remains to be actual. One of the possible ways can be found in application of gated structures with externally tuned periodic electric potential.

In our recent paper we studied quantum states and the electron spin distribution in a system combining the spin-splitting phenomena caused by the SO interaction and the external gate-controlled periodic electric potential.<sup>19</sup> We investigated the Bloch spinors and spin polarization that can be achieved in currently manufactured gated semiconductor structures with lateral superlattice. Such 1D superlattice can be fabricated by the metal-gate evaporation with typical period of 50–200 nm. We use the value of lateral period in the x-direction to be  $a = 60$  nm which this gives the energy scale  $\hbar^2/2ma^2$  to be of the order of 10 meV for the effective mass  $m = 0.036m_0$  in InAs. Such energy scale is comparable to the characteristic SO energy in two-dimensional InAs-based structure where the Rashba coupling constant reaches its biggest value 3:4  $\times 10^1$  eV m observed in the experiments.<sup>20</sup> It should be mentioned that the energy scale of 10 meV means that the effects in SO superlattices discussed here

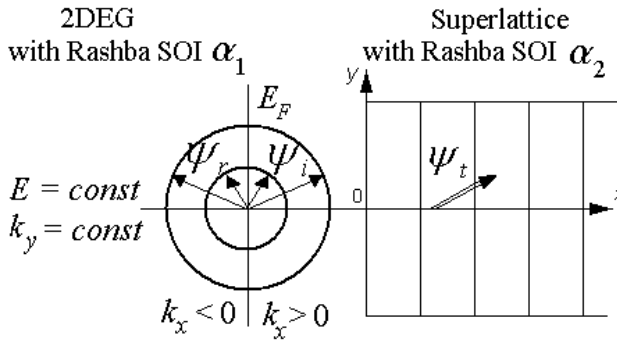


FIG. 1: Geometry of scattering of 2D EG with Rashba SO interaction on the spin-orbit lateral superlattice. The incoming  $\psi_i$  and reflected  $\psi_r$  spinors are the eigenstates of Rashba Hamiltonian with spin-orbit coupling constant  $\alpha_1$  and wavevectors belonging to the same Fermi contour. The transmitted states  $\psi_t$  are the Bloch spinors corresponding to another spin-orbit coupling constant  $\alpha_2$ .

can be clearly observed experimentally at helium temperatures. In the present paper we make an extensive use of our results for the quantum states in SO superlattice<sup>19</sup> for investigation of the problem of scattering for 2D EG with Rashba SO coupling on the SO superlattice. We solve the scattering problem on the SO superlattice occupying a half-space and study the transmitted states as a function of the Fermi energy of the incoming states. For the transmitted states the space distribution of spin density components is calculated for different values of Rashba coupling on both sides of the interface, for various amplitudes of the periodic potential and Fermi level position in the 2D EG.

The paper is organized as follows. In Sec. II we formulate the scattering problem and describe the incoming, reflected, and transmitted states. We also briefly discuss the structure of the eigenstates of the SO superlattice. In Sec. III the space distribution of spin density in the transmitted state is calculated, and different cases of Rashba coupling on both sides of the interface are discussed. The concluding remarks are given in Sec. IV.

## II. THE SCATTERING PROBLEM

We consider the scattering of electrons with spin-orbit coupling constant  $\alpha_1$  on the one-dimensional superlattice occupying a half-space  $x > 0$  and also having a spin-orbit Rashba term with another value of Rashba coupling constant  $\alpha_2$ . The incoming and reflected spinors are the eigenstates of Rashba Hamiltonian and belong to the same Fermi energy of the 2D electron gas. The transmitted states are the Bloch spinors with each of the components possessing the Bloch theorem. In addition to the energy, the  $k_y$  component of the momentum is conserved since the system is homogeneous in the  $y$  direction, as it is shown schematically in Fig. 1.

The half-space  $x < 0$  is the semiconductor structure with 2D EG characterized by the effective mass  $m$  and Rashba spin-orbit coupling strength  $\alpha_1$ . The quantum states here are the eigenstates of the Hamiltonian ( $\hbar = 1$ )

$$\hat{H}_0 = \frac{\hat{p}^2}{2m} + \alpha_1 (\hat{p}_x \hat{p}_y - \hat{p}_y \hat{p}_x) : \quad (1)$$

The eigenstate of (1) labeled by the momentum  $k_0 = (k_x; k_y)$  and the polarization index  $\sigma = \pm 1$  has the following form:

$$x < 0 : \quad \psi_i = \frac{e^{ik_0 \cdot r}}{2} \frac{1}{e^{\pm i\sigma_0}} \quad (2)$$

where  $\sigma_0 = \arg [k_y - ik_x]$ , and the energy of the state is

$$E_0(k; \sigma) = \frac{k^2}{2m} + \alpha_1 k : \quad (3)$$

The value  $\sigma = 1$  labels the state with negative  $y$  projection of the spin for positive  $k_x$  and  $k_y = 0$  and thus it is usually described as Rashba "down" polarized state while the value  $\sigma = -1$  labels the Rashba "up" polarized state. It should be mentioned that the state (2) does not exhibit any spin texture, i.e. it has a uniform space distribution of all spin density components  $S_i = \hat{S}_i$

$$S_x = \cos \sigma_0; \quad S_y = \sin \sigma_0; \quad S_z = 0: \quad (4)$$

The idea of the system setup in Fig. 1 is to convert such uniform distribution into a non-trivial spin texture by using a superlattice.

The incoming state is scattered on the border of the SO superlattice occupying the area at  $x > 0$ . In the left part of the space  $x < 0$  there is the reflected state which is the linear combination of all eigenstates of (1) with the same energy as the incoming state and with  $k_x < 0$  since the reflected states are moving to the left. Since the Rashba Hamiltonian (1) is two-fold degenerate both for  $k_x > 0$  or  $k_x < 0$ , the reflected state consists of two spinors with the same energy as the incoming state but with different  $k_x$  momenta belonging to different branches of Rashba Hamiltonian (1) with  $\sigma = \pm 1$  (see Fig. 1). The wavevector modulus  $k_{1,2}$  at fixed energy can be found from (1) and are equal to

$$k_{1,2} = \sqrt{\frac{2mE + (\alpha_1)^2}{m}} \quad m \quad (5)$$

where  $\pm$  and  $\mp$  refer to the down- and up-Rashba bands with  $\sigma = \pm 1$ . The  $k_x$  component for each  $k_{1,2}$  at fixed  $k_y$  is given by the usual relation  $k_{1,2x} = \sqrt{k_{1,2}^2 - k_y^2}$ . Thus, the reflected state at  $x < 0$  has the following form:

$$x < 0 : \quad r = r_1 \frac{e^{ik_1 x + ik_y y}}{p - \frac{2}{2}} \quad \frac{1}{e^{i_1}} + \\ + r_2 \frac{e^{ik_2 x + ik_y y}}{p - \frac{2}{2}} \quad \frac{1}{e^{i_2}} : \quad (6)$$

Here the phases are defined by the momentum components as  $i_{1,2} = \arg [k_y - ik_{1,2}x]$  and  $r_{1,2}$  are the reflection coefficients which will be found below.

On the right-hand side in Fig.1 at  $x > 0$  the transmitted electrons travel through the SO superlattice. The transmitted state is the linear combination of the eigenstates of the SO superlattice with the energy and  $k_y$  equal to those of the incoming state:

$$x > 0 : \quad t = \sum_j c_j (k_j; k_y) \quad (7)$$

where the coefficients  $c_j$  can be found from the boundary conditions and  $(k_j; k_y)$  are the eigenstates of the SO superlattice. Here we shall briefly describe the structure of these states which were studied previously in more details.<sup>19</sup>

The Hamiltonian for the SO superlattice is the sum of the Rashba Hamiltonian (1) and the one-dimensional periodic potential  $V(x)$  of a 1D superlattice with the period  $a$ . The simplest approximation for the form of the periodic potential can be chosen as

$$V(x) = V_0 \cos \frac{2\pi x}{a} : \quad (8)$$

The wavefunction can be constructed as a superposition of two-component spinors (2) which are the eigenstates of the Rashba Hamiltonian (1). In the presence of the periodic potential the wavevectors of the basis states are shifted by the reciprocal lattice vector  $b$  of the superlattice:

$$k_n = k + nb = k_x + \frac{2\pi}{a} n; \quad k_y ; \quad (9)$$

$n = 0, 1, 2, \dots$ . The eigenstate thus has the form

$$s_k = \sum_n a_n^s (k) \frac{e^{ik_n r}}{p - \frac{2}{2}} \quad \frac{1}{e^{i_n}} ; \quad = 1 \quad (10)$$

where  $k$  is the quasimomentum in the 1D Brillouin zone,  $s$  is the band number, and  $i_n = \arg [k_y - ik_{nx}]$ . After substituting the wavefunction (10) into the Schrödinger equation the coefficients  $a_n^s$  are determined by the standard eigenvalue problem. The transmitted state (7) is the superposition of Bloch spinors (10) with different quasimomentum components  $k_x = k_j$  for which the energy is equal to the energy of the incident wave, and with the

same  $k_y$  momentum component as in the incident wave since the structure is homogeneous along the  $y$  direction.

The scattering on the interface at  $x = 0$  is described by the boundary conditions. For the problem considered in the paper these conditions have the form of the continuity equations which follow from the Schrödinger equation and can be written as

$$j_{x=0} = j_{x=0+} ; \quad (11)$$

$$\hat{v}_x j_{x=0} = \hat{v}_x j_{x=0+} \quad (12)$$

where

$$\hat{v}_x = \frac{\partial \hat{H}}{\partial k_x} = \frac{\hat{p}_x}{m} \quad \hat{v}_y : \quad (13)$$

The equations (12) link the wavefunction  $r$  at the left half-space  $x < 0$  and the wavefunction  $t$  at the right half-space  $x > 0$ . Since both of the equations in (12) are written for two-component spinors, one has a system of four algebraic inhomogeneous equations describing the scattering which can be easily solved.

The quantum numbers which remain to be good during the scattering on 1D superlattice with the potential (8) are the  $k_y$  component of the momentum and the energy of the incoming state. Here one has to distinguish the case when the energy of the incoming state at fixed  $k_y$  is within the limits of one of the superlattice bands and when this energy corresponds to a gap in the superlattice spectrum. The first case corresponds to the solution of system (12). For the second case the solution to the Schrödinger equation is not finite on the whole  $x$  axis and thus there are no states which propagate from the scattering interface through the superlattice. We call such case as a case of total reflection in analogy with optical scattering. It should be mentioned that such effect was already observed for the scattering of the Rashba states on the interface between two areas with different SO constant.<sup>17</sup> The states which do not propagate through the superlattice and are localized at the interface border are known as Tam states. Such states were studied previously both in bulk crystals<sup>21,22</sup> and later in the superlattices.<sup>23,24,25</sup> In the latter case it was shown that typically the Tam states decay inside the superlattice on the length of several periods with different results varying from two - three<sup>23</sup> to five - seven<sup>25</sup> lattice periods. In our case these results mean that the typical penetration length of Tam states will be of the order of 100 - 700 nm which is substantially smaller than the total length of superlattices actually used in the present experiments. Hence, there will be no detection of such states with the possible device mounted after the superlattice. Thus, we neglect the Tam states localized at the interface and consider only the Bloch states with the energy belonging to the bands of the superlattice which were discussed above.

### III. SPIN TEXTURE OF THE TRANSMITTED STATE

When the transmitted state (7) is fully determined, one can calculate the space distribution of the spin density  $\hat{y}^i$  for the transmitted state which depends on the wavevector and polarization of the incident state (2). In a real experimental setup of 2D EG structure the electrons occupy not a single state with a given wavevector and polarization but all of the states on the Fermi level, as it is shown schematically in Fig.1. The electrons with  $k_x > 0$  travel to the scattering interface and take part in the scattering process. Thus, it is reasonable to calculate the spin density for all the electrons with a chosen Fermi energy and  $k_x > 0$  giving us the spin density distribution which can be actually probed by a detector,

$$S_i(x; y) = \int_{k_F x > 0} \hat{y}^i \, t \, dk : \quad (14)$$

Since the system is homogeneous in the  $y$  direction, one may consider only the  $x$ -dependence of (14) which may show some non-trivial spin texture along the superlattice. As it was mentioned above, the incident state of 2D EG with Rashba spin-orbit coupling has a space-independent spin density distribution (4). Below we shall see that a non-uniform spin density distribution which can be actually probed by a detector may be created by scattering on the SO superlattice.

First, let us assume equal values of the Rashba coupling constant in the InAs-based 2D EG and in the SO superlattice  $\lambda_1 = \lambda_2 = 3 \times 10^1$  eV nm. The  $x$ -dependence of the spin texture is shown in Fig.2 for the Fermi energy of 2D EG equal to 10 m eV in Fig.2(a) and to 20 m eV in Fig.2(b), with the amplitude of the periodic potential  $V_0 = 2$  m eV. The upper plot on each figure shows the  $(S_x; S_z)$  projections of the spin density (14) while the lower one demonstrates the space dependence of  $(S_x; S_y)$  components. The space distance on the plot is measured in units of superlattice period  $a = 60$  nm and starts at  $n = 1$  which means that the spin detector is located far away from the superlattice border.

The spin texture in Fig.2 has several remarkable features. First of all, it has a non-zero component  $S_z$  which is absent in spin density (4) of the uniform 2D EG with Rashba SO coupling. For the spin expectation values  $\langle \hat{S}_i \rangle = \int S_i \, dk$  calculated for our problem one has in general

$$x = z = 0; \quad y \neq 0 \quad (15)$$

which follows from the symmetry considerations of the system (see Fig.1). Indeed, the system is symmetrical with respect to  $y$  sign reversal which means for Rashba SO coupling that  $x = 0$ . The Rashba SO interaction also can not create the  $z$  polarization of 2D EG and thus  $z = 0$ , as in the initial state. It should be noted that

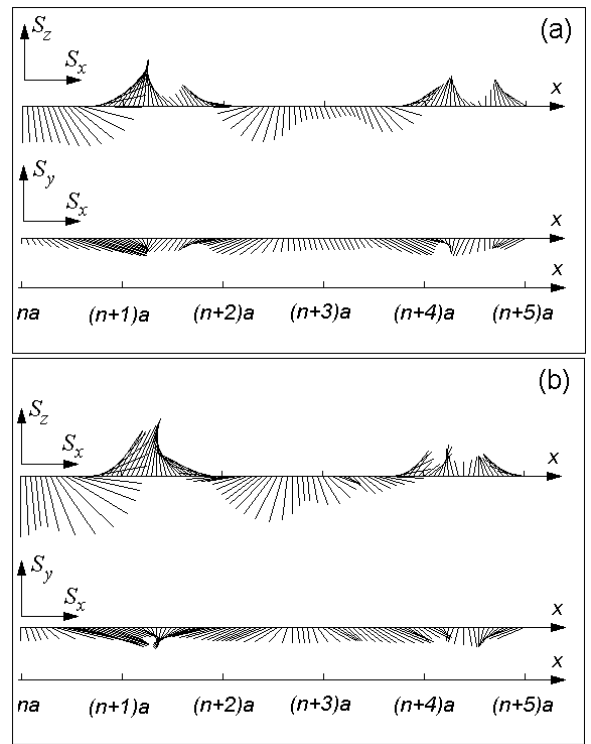


FIG. 2: Spin texture in transmitted state distributed along the superlattice for the equal Rashba constant  $\lambda = 3 \times 10^1$  eV nm inside and outside the superlattice. The periodic potential amplitude  $V_0 = 2$  m eV and the Fermi energy is (a)  $E_F = 10$  m eV, (b)  $E_F = 20$  m eV. The distance is measured in units of superlattice period  $a = 60$  nm and starts at  $n = 1$  far away from the border. The superlattice acts as a spin flip device which converts the uniformly distributed spins in the incident wave to the spin textured state inside the superlattice.

a similar feature was observed previously for the eigenstates in the SO superlattices at given quantum numbers  $(k_x; k_y)$  in the Brillouin zone.<sup>19</sup> The only symmetry breaking caused by the scattering interface cancels the  $x$  sign reversal symmetry, making only the states with  $k_x > 0$  to be actually scattered. Thus, one can see in Fig.2 and below in Fig.4 that one sign of  $S_y(x)$  dominates, leading in those cases to a nonzero expectation value  $\langle \hat{y} \rangle$ . The other reason is that the contributions to the spin expectation value  $\langle \hat{y} \rangle$  from two parts of Fermi contours of the Rashba bands with  $k_x = 1$  (see Fig.1) do not compensate each other due to the distance  $2m_1$  between the Fermi radii, as it is seen from (5). Another interesting feature of the spin density distribution in Fig.2 is that it does not repeat itself on the distance of one superlattice period. The explanation is that the transmitted state (7) consists of the Bloch spinors with different  $k_x$  components of the quasimomentum. As one can see from Fig.2, the approximate space period for the spin density is about several superlattice periods and, as our calculations have shown, does not depend on partic-

ular starting point  $x = na$  if condition  $n \geq 1$  is satisfied. The latter means that the spin density detector is located far away from the scattering border, as it is supposed to be in real experiments. This circumstance allows to neglect the influence of the second right-hand border of the superlattice while solving the scattering problem.

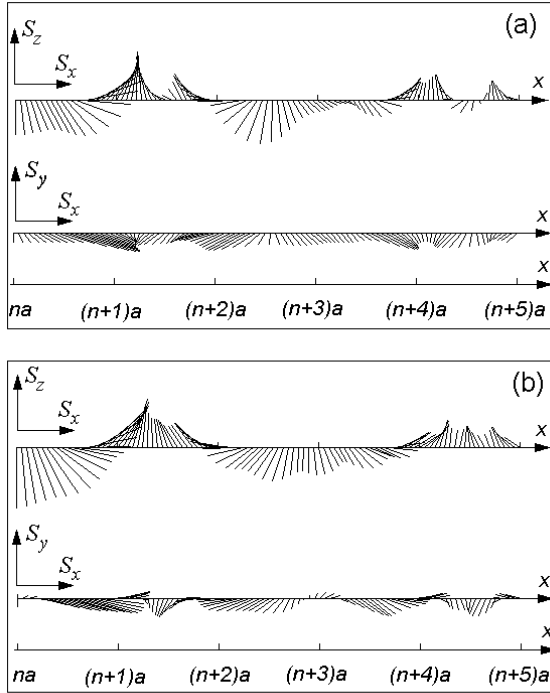


FIG. 3: Spin texture along the superlattice for the Rashba constant  $\tau_2 = 3 \cdot 10^1$  eV m inside and  $\tau_1 = 0.1 \cdot \tau_2$  outside the superlattice. The periodic potential amplitude  $V_0 = 5$  m eV and the Fermi energy is (a)  $E_F = 10$  m eV and (b)  $E_F = 30$  m eV. The  $S_y$  spin texture in (b) corresponds to the smaller expectation value than the one in Fig. 2 since two parts of the Fermi contours are closer to each other at  $\tau_1 = 0.1 \cdot \tau_2$  and their spin polarizations are almost canceled.

Let us now consider a case when the Rashba coupling constant  $\tau_1$  in the 2DEG on the left is substantially smaller than the parameter  $\tau_2$  in the superlattice. This situation corresponds, for example, to the GaAs-based structure attached to the InAs-based SO superlattice. The results for the spin density distribution along the superlattice for  $\tau_1 = 0.1 \cdot \tau_2$  are shown in Fig. 3 for the amplitude of the periodic potential  $V_0 = 5$  m eV and for the same values of the Fermi energy  $E_F = 10$  m eV and  $E_F = 30$  m eV of the incident state. By comparing Fig. 3 and Fig. 2 one can see that qualitatively the pattern of the spin texture for  $\tau_1 = 0.1 \cdot \tau_2$  and for the bigger  $V_0$  is similar to the one for the equal SO parameters. The reason for this is that the spin density (14) shown in Fig. 3 and Fig. 2 is an integral characteristic of the scattering process and thus it is less sensitive to the system parameters than, for example, the transmission coefficient for the state with one particular chosen angle of incidence.<sup>17</sup>

However, there are qualitative differences at high Fermi energies in the  $S_y$  component distributions. Comparing Fig. 2b and Fig. 3b, one can see that the latter corresponds to a substantially smaller magnitude of the expectation value  $y = \langle S_y(x) \rangle dx$  because the spin density  $S_y$  provides both positive and negative contributions. Such difference is caused by the smaller Rashba parameter  $\tau_1$  on Fig. 3 compared to Fig. 2b which leads to the closer placement of two parts of the Fermi contours in the  $k$ -space (see Fig. 1). Hence, their contributions to the spin expectation values leads to the smaller  $y$  in addition to the precise cancellation of  $S_x$  and  $S_z$ .

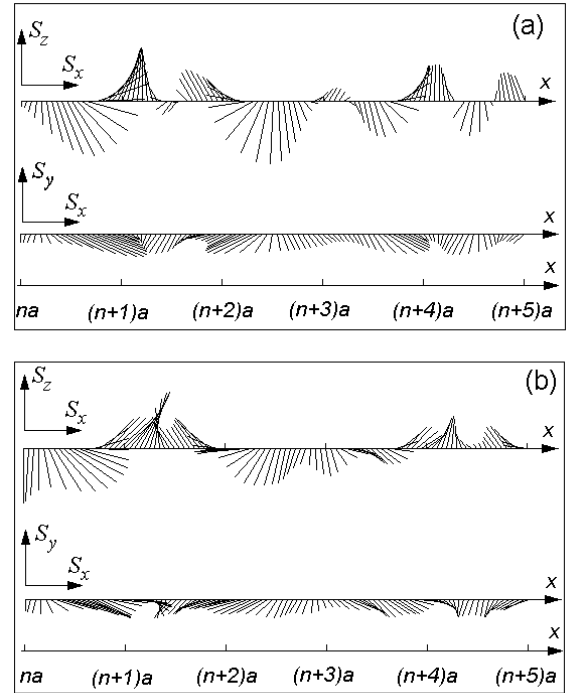


FIG. 4: Spin texture along the superlattice for the Rashba constant  $\tau_1 = 3 \cdot 10^1$  eV m outside and  $\tau_2 = 0.1 \cdot \tau_1$  inside the superlattice. The periodic potential amplitude  $V_0 = 5$  m eV and the Fermi energy is (a)  $E_F = 10$  m eV and (b)  $E_F = 30$  m eV. The pattern of the spin texture is similar to the one for equal SO parameters shown in Fig. 2 due to the same spin-orbit coupling in the incident state.

Finally we turn our attention to the opposite case  $\tau_2 = 0.1 \cdot \tau_1$  which can be realized experimentally, for example, by the GaAs-based SO superlattice attached to the InAs-based 2DEG. The results for the spin density distributions are presented in Fig. 4. Again one can see the similarity between all the spin density textures in Fig. 4, Fig. 3 and Fig. 2. The initial state in Fig. 4 has the same value of Rashba coupling strength as in Fig. 2 which leads qualitatively to a similar shape for all spin density components including  $S_y$ . The integral spin density distribution (14) maintains qualitatively the same form for different values of system parameters since it is sensible only to the global characteristics of the energy

spectrum of the superlattice which remain unchanged under variation of the Rashba coupling strength and periodic potential amplitude. Such robust spin density shape indicates that the effects discussed in the paper should survive under various perturbations which were left out of the scope in the present work such as defects and finite temperature. This conclusion can be justified further if we mention that the energy scale of the problem studied above belongs to the interval of  $10 \text{--} 30 \text{ meV}$ , which means that the effects discussed in the paper should be clearly observable at helium, and possibly also at nitrogen temperatures.

#### IV. CONCLUSIONS

We have studied the scattering of two-dimensional electron gas on the one-dimensional superlattice where the spin-orbit coupling was taken into account for both systems. The space distribution of spin density components

was calculated for different values of Rashba coupling on both sides of the interface, for various amplitudes of the periodic potential and Fermi level position. The observed shape of spin density standing waves is found to be insensitive to particular values of the electron Fermi energy and the strength of periodic potential, indicating that the effects discussed in the paper should survive under various perturbations such as defects and finite temperature. The scale of energy involved in the processes discussed in the paper makes the results to be promising for experimental observation.

#### Acknowledgments

The author thanks V.Ya. Demikhovskii for numerous fruitful discussions. The work was supported by the RNP Program of the Ministry of Education and Science RF, by the RFBR, CRDF, and by the Foundation "Dynasty" - ICFPM.

Electronic address: khomitsky@phys.unn.ru

- <sup>1</sup> E.I. Rashba, *Fiz. Tverd. Tela* (Leningrad) 2, 1224 (1960) [Sov. Phys. Solid State 2, 1109 (1960)]; Y.A. Bychkov and E.I. Rashba, *J. Phys. C* 17, 6039 (1984).
- <sup>2</sup> I. Zutic, J. Fabian, and S. Das Sarma, *Rev. Mod. Phys.* 76, 323 (2004).
- <sup>3</sup> S. Das Sarma and B. Das, *Appl. Phys. Lett.* 56, 665 (1990).
- <sup>4</sup> A.V. Moroz and C.H.W. Barnes, *Phys. Rev. B* 60, 14272 (1999).
- <sup>5</sup> F. Mireles and G. Kirczenow, *Phys. Rev. B* 64, 024426 (2001).
- <sup>6</sup> M. Governale and U. Zulicke, *Phys. Rev. B* 66, 073311 (2002).
- <sup>7</sup> X.F. Wang and P. Vasilopoulos, *Phys. Rev. B* 67, 085313 (2003).
- <sup>8</sup> X.F. Wang, P. Vasilopoulos, and F.M. Peeters, *Phys. Rev. B* 65, 165217 (2002).
- <sup>9</sup> X.F. Wang, *Phys. Rev. B* 69, 035302 (2004).
- <sup>10</sup> S. Debaud and B. Kramer, *Phys. Rev. B* 71, 115322 (2005).
- <sup>11</sup> P. Kleinert, V.V. Bryksin, O. Leiberman, *Phys. Rev. B* 72, 195311 (2005).
- <sup>12</sup> L. Zhang, P. Brusheim, and H.Q. Xu, *Phys. Rev. B* 72, 045347 (2005).
- <sup>13</sup> A. Reynoso, G. Uso, and C.A. Balseiro, *Phys. Rev. B* 73, 115342 (2006).

- <sup>14</sup> J.B. Miller, D.M. Zumbuhl, C.M. Marcus, Y.B. Lyanda-Geller, D.G. Goldhaber-Gordon, K. Campbell, and A.C. Gossard, *Phys. Rev. Lett.* 90, 076807 (2003).
- <sup>15</sup> V.Ya. Demikhovskii and A.A. Perov, *Europhys. Lett.* 76, 477 (2006).
- <sup>16</sup> M. Langenbuch, M. Suhre, and U. Rossler, *Phys. Rev. B* 69, 125303 (2004).
- <sup>17</sup> M. Khodas, A. Shekhter, and A.M. Finkel'stein, *Phys. Rev. Lett.* 92, 086602 (2004).
- <sup>18</sup> A. Shekhter, M. Khodas, and A.M. Finkel'stein, *Phys. Rev. B* 71, 125114 (2005).
- <sup>19</sup> V.Ya. Demikhovskii and D.V. Khomitsky, *JETP Letters* 83, iss.8, p.340 (2006) [*Pis'ma v ZhETF* 83, iss.8, p.399 (2006)].
- <sup>20</sup> D. Grunder, *Phys. Rev. Lett.* 84, 6074 (2000).
- <sup>21</sup> E.T. Goodwin, *Proc. Cambridge Philos. Soc.* 35, 221 (1939).
- <sup>22</sup> S.D. Kevan, N.G. Stoel, and N.V. Smith, *Phys. Rev. B* 32, 4956 (1985).
- <sup>23</sup> H. Ohno, E.E. Mendez, J.A. Brum, J.M. Hong, F. Aigol-Rueda, L.L. Chang, and L. Esaki, *Phys. Rev. Lett.* 64, 2555 (1990).
- <sup>24</sup> H.K. Sy and T.C. Chua, *Phys. Rev. B* 48, 7930 (1993).
- <sup>25</sup> J.K. Los and H. Puszkarzki, *Phys. Rev. B* 68, 045316 (2003).